J Physiol 591.19 (2013) pp 4877–4894

JPn Neuroscience The Journal of Physiology

Modulation of synaptic depression of the calyx of Held synapse by $GABA_B$ receptors and spontaneous activity

Tiantian Wang[1], Silviu I. Rusu[1], Bohdana Hruskova[2], Rostislav Turecek[2] and J. Gerard G. Borst[1]

[1] *Department of Neuroscience, Erasmus MC, University Medical Center Rotterdam, The Netherlands*
[2] *Department of Auditory Neuroscience, Institute of Experimental Medicine ASCR, 14220 Prague, Czech Republic*

Key points

- Spontaneous activity contributes to low synaptic depression of the calyx of Held synapse *in vivo*.
- Application of a reversible blocker in combination with juxtacellular recordings allows a relatively good estimate of local drug concentrations reached during microiontophoresis.
- Activation of the $GABA_B$ receptor on the young-adult calyx of Held can reduce short-term depression, both *in vivo* and in slices.
- The ambient concentration of GABA in the auditory brainstem is low.

Abstract The calyx of Held synapse of the medial nucleus of the trapezoid body is a giant axosomatic synapse in the auditory brainstem, which acts as a relay synapse showing little dependence of its synaptic strength on firing frequency. The main mechanism that is responsible for its resistance to synaptic depression is its large number of release sites with low release probability. Here, we investigated the contribution of presynaptic $GABA_B$ receptors and spontaneous activity to release probability both *in vivo* and *in vitro* in young-adult mice. Maximal activation of presynaptic $GABA_B$ receptors by baclofen reduced synaptic output by about 45% in whole-cell voltage clamp slice recordings, which was accompanied by a reduction in short-term depression. A similar reduction in transmission was observed when baclofen was applied *in vivo* by microiontophoresis during juxtacellular recordings using piggyback electrodes. No significant change in synaptic transmission was observed during application of the $GABA_B$ receptor antagonist CGP54626 both during *in vivo* and slice recordings, suggesting a low ambient GABA concentration. Interestingly, we observed that synapses with a high spontaneous frequency showed almost no synaptic depression during auditory stimulation, whereas synapses with a low spontaneous frequency did depress during noise bursts. Our data thus suggest that spontaneous firing can tonically reduce release probability *in vivo*. In addition, our data show that the ambient GABA concentration in the auditory brainstem is too low to activate the $GABA_B$ receptor at the calyx of Held significantly, but that activation of $GABA_B$ receptors can reduce sound-evoked synaptic depression.

(Received 13 April 2013; accepted after revision 7 August 2013; first published online 12 August 2013)
Corresponding author J. G. G. Borst: Department of Neuroscience, Erasmus MC, University Medical Center Rotterdam, Dr. Molewaterplein 50, 3015 GE Rotterdam, The Netherlands. Email: g.borst@erasmusmc.nl

Abbreviations aCSF, artificial cerebrospinal fluid; eAP, amplitude of the extracellularly recorded action potential; eEPSP, amplitude of the extracellularly recorded excitatory postsynaptic potential; eEPSP′, maximum rate of rise of eEPSP; MNTB, medial nucleus of the trapezoid body; PSTH, peristimulus time histogram; STD, short-term depression.

DOI: 10.1113/jphysiol.2013.256875

Introduction

Each principal neuron in the medial nucleus of the trapezoid body (MNTB) is contacted by a single, giant axosomatic terminal called the calyx of Held. Because of its accessibility for patch-clamp recordings, the calyx of Held synapse has been used extensively to study the mechanisms of short-term plasticity in slice recordings (von Gersdorff & Borst, 2002). However, it was recently shown that this synapse displays only little short-term plasticity *in vivo* after hearing onset (Lorteije *et al.* 2009; Crins *et al.* 2011; Sonntag *et al.* 2011), which is in line with its adult function as a relay synapse. Short-term depression (STD) is developmentally regulated, and its impact is strongly reduced after hearing onset (Crins *et al.* 2011). The low release probability at its large number of release sites seems to be the main reason for the reduced STD observed in the mature calyx (Taschenberger & von Gersdorff, 2000; Iwasaki & Takahashi, 2001; Taschenberger *et al.* 2002). A low quantal output was also observed during *in vivo* recordings of the mature calyx for which, apart from the developmental reduction in release probability, the low extracellular calcium concentration *in vivo* compared to formulas typically used in slice experiments was also an important factor (Lorteije *et al.* 2009). At hearing onset, the firing pattern of this synapse switches from a bursting firing pattern to the primary-like firing pattern of the adult synapse (Sonntag *et al.* 2009; Tritsch *et al.* 2010), with an average firing frequency of about 30 Hz (Spirou *et al.* 1990; Kopp-Scheinpflug *et al.* 2008). Results from slice experiments have suggested that the typically high spontaneous activity will depress this synapse *in vivo* (Hermann *et al.* 2007, 2009; Lorteije *et al.* 2009), which would be another cause for the observed low quantal output *in vivo*.

Despite the simple relay function of the calyx of Held synapse, which allows principal neurons of the MNTB to provide inhibition that is both well timed and sustained to many other auditory nuclei, glutamate release from the calyx of Held is modulated by a number of neurotransmitters. The strongest modulator is GABA, acting via presynaptic $GABA_B$ receptors. Presynaptic $GABA_B$ receptors are also prominently present at other auditory brainstem nuclei (reviewed in Grothe & Koch, 2011). Activation of $GABA_B$ receptors can block at least 80% of transmitter release, among others by reducing the presynaptic Ca^{2+} current (Isaacson, 1998; Takahashi *et al.* 1998; Wu *et al.* 1998) via an action of β/γ G-protein subunits (Kajikawa *et al.* 2001). Block of the Ca^{2+} channels is voltage-sensitive, and is accompanied by a slowing of the Ca^{2+} channel activation (Isaacson, 1998). In addition, GABA can directly interfere with the vesicle cycle by lowering cAMP (Sakaba & Neher, 2003).

Presynaptic $GABA_B$ receptors generally have high affinity for GABA (Yoon & Rothman, 1991). We therefore hypothesized that an additional explanation for the difference in the amount of synaptic depression between *in vivo* and slices might be that the extracellular GABA concentration is higher *in vivo* than in slices, as bath perfusion may reduce the ambient GABA concentration (Hájos & Mody, 2009). Although estimates of the ambient GABA concentrations range between 100 and 800 nM (Lerma *et al.* 1986; Tossman *et al.* 1986; Dvorzhak *et al.* 2010), close to the predicted theoretical minimum (Attwell *et al.* 1993), the $GABA_B$ receptor can already be tonically activated in slices (Emri *et al.* 1996; Kombian *et al.* 1996; Le Feuvre *et al.* 1997; Lin & Dun, 1998; Aroniadou-Anderjaska *et al.* 2000; Kirmse & Kirischuk, 2006; Wu *et al.* 2011), and large tonic inhibition has been observed *in vivo* in the olfactory bulb (Pírez & Wachowiak, 2008). Here, we therefore investigate whether the presynaptic $GABA_B$ receptor of the young-adult calyx of Held is tonically activated in slices or *in vivo*. In addition, we test the impact of spontaneous activity and $GABA_B$ receptor activation on short-term plasticity.

Methods

Ethical approval

All experiments were conducted in accordance with the European Communities Council Directive and were approved by the Animal Ethics Committee of the Erasmus MC.

Animals and surgery

After brief exposure to isoflurane, the adult C57BL/6 mice (35–60 days old) were injected I.P. with a ketamine–xylazine mixture (65 and 10 mg kg^{-1}, respectively). A homeothermic blanket (FHC, Bowdoinham, ME, USA) was used to keep the rectal body temperature at 37°C. Animals were supine positioned, with their heads immobilized by a metal pedestal glued to the dorsal skull. A tracheotomy was performed and the animal was ventilated mechanically with oxygen (MiniVent; type 845; Hugo Sachs Elektronik - Harvard Apparatus GmbH, March-Hugstetten, Germany). Ventilation frequency was about 150 min^{-1}; stroke volume was 7 μl (g body weight)$^{-1}$. The right MNTB was accessed via ventral surgery as previously described, using the right anterior inferior cerebellar artery and basilar artery as landmarks to locate the MNTB (Rodriguez-Contreras *et al.* 2008; Crins *et al.* 2011). Both the dura and the pia were removed to expose the brain surface before recording. Ringer solution (containing (in mM): NaCl 135, KCl 5.4, $MgCl_2$ 1, $CaCl_2$ 1.8, Hepes 5 (pH 7.2)) was applied to keep the brain surface moist.

In vivo electrophysiology and pharmacology

Recordings from principal neurons were made with the *in vivo* juxtacellular (loose-patch) recording technique, using thick-walled borosilicate glass micropipettes with filament, which were filled with Ringer solution, as described previously (Lorteije *et al.* 2009). The recording pipette penetrated the brain surface with a positive pressure of 300 mbar. The pressure was reduced to ∼30 mbar after passing the brain surface, and to 0 mbar when recording started. Data were acquired with a MultiClamp 700B patch-clamp amplifier and pCLAMP 9.2 software (MDS Analytical Technologies, Sunnyvale, CA, USA), filtered at 10 kHz (eight-pole Bessel filter), and sampled at 50 kHz with a 16-bit A/D converter (Digidata 1322A).

Juxtacellular recordings were combined with local drug application by gluing the recording pipette to a five-barrel micropipette (5B120F-4; World Precision Instruments, Inc., Sarasota, FL, USA) in a 'piggy-back' configuration (Havey & Caspary, 1980). The distance between the tip of the recording electrode and the tips of the multibarrel electrode was about 50 μm. In most experiments, the five barrels of the iontophoretic micropipette were filled with: 160 mM EGTA, 10 mM (±)-baclofen (Ascent, Avonmouth, UK; pH 3 with HCl after dissolving in 0.9% saline), 1 mM CGP54626 hydrochloride (Tocris Bioscience, Ellisville, MO, USA), 0.9% NaCl (pH 3 with HCl) and 0.9% NaCl (pH 7.2). EGTA was dissolved in distilled water adjusted to pH 10 with NaOH. After dissolving, the EGTA solution was adjusted to a final pH of 7.2. CGP54626 was stored at −20°C as a 100 mM stock solution in DMSO, and diluted to 1 mM in 0.9% NaCl and adjusted to pH 3 with HCl. The barrel containing 0.9% NaCl at pH 7.2 served as a sum channel for automatic current balancing. The barrels were connected by AgCl wire to an iontophoresis current generator (Dagan 6400 Advanced; Minneapolis, MN, USA).

Auditory stimulation

Closed field sound stimulation was presented as described previously (Tan & Borst, 2007). A speaker probe was inserted into the left ear canal and was stabilized with silicone elastomer. A two-noise-burst stimulation protocol was designed in MATLAB (Version R2008a), and the auditory stimulus was generated by Tucker Davis Technologies hardware (TDT, system 3, RX6 processor, PA5.1 attenuator, ED1 electrostatic driver, EC1 electrostatic speaker; Alachua, FL, USA). Clampex acquisition was triggered at the same time by MATLAB as the auditory stimulation program. This protocol consists of a 200 ms silent period, followed by two 400 ms bursts of wide band noise (bandwidth 2–40 kHz; 80 dB SPL) which were presented at six different intervals (40, 80, 160, 320, 640, 1280 ms), followed by a silent period for a total sweep duration of 4 s. Sound intensities were calibrated as previously described (Tan & Borst, 2007). During drug application this protocol was continuously played, allowing an assessment of the effect on both spontaneous and sound-evoked events. Experiments were performed in a single-walled sound attenuated chamber (Gretch-Ken Industries, Lakeview, OR, USA).

Preparation of slices

Slices were prepared as previously described (Lorteije *et al.* 2009). Young-adult C57BL/6 mice aged P24–30 (P0 defined as the day of birth) were decapitated following isoflurane anaesthesia. The brainstem was dissected in ice-cold saline containing (in mM): 125 NaCl, 2.5 KCl, 3 $MgSO_4$, 0.1 $CaCl_2$, 1.25 NaH_2PO_4, 0.4 ascorbic acid, 3 *myo*-inositol, 2 pyruvic acid, 25 D-glucose, 25 $NaHCO_3$ (Merck, Darmstadt, Germany), prebubbled with 95% O_2/5% CO_2, pH 7.4. Coronal slices containing the MNTB were cut at 150 or 200 μm in ice cold saline using a vibratome (Vibratome, St. Louis, MO, USA). After slicing, the tissue was incubated for 30 min at 37°C in a holding chamber containing artificial cerebrospinal fluid (aCSF) with the same composition as the slicing solution, except that the concentration of $CaCl_2$ and $MgCl_2$ were 2 and 1 mM, respectively (standard slice conditions). Afterwards, slices were kept at room temperature until the time of recording.

Electrophysiological recordings

For recording, slices were placed in the holding chamber of an upright microscope (BX-50; Olympus, Tokyo, Japan) and MNTB principal cells were visualized using a 40× water immersion objective. Slices were continuously perfused with oxygenated aCSF maintained at physiological temperature (35–37°C) using a perfusion heater.

During electrophysiological recordings the $CaCl_2$ concentration of the aCSF was lowered to 1.2 mM. To activate GABA$_B$ receptors, baclofen was dissolved in the aCSF containing 1.2 mM $CaCl_2$ to a concentration of 100 μM. In some experiments, the aCSF was supplemented with 10 μM CGP54626 either alone or in combination with 100 μM baclofen, to test for the effects of tonic GABA$_B$ receptor activation on short-term plasticity. Extracellular solutions were exchanged with a four-channel peristaltic pump (RP-1; Rainin Instrument Co., San Diego, CA, USA) using manually controlled valves.

Whole cell voltage clamp recordings were performed using borosilicate glass pipettes (3–5 MΩ) filled with intracellular solution containing (in mM): 126 potassium gluconate, 20 KCl, 10 Na_2-phosphocreatine, 4 MgATP,

0.3 Na_2GTP, 0.5 EGTA and 10 Hepes (310 mmol kg^{-1}), pH 7.2.

Recordings were performed in whole cell voltage-clamp configuration. The holding voltage was set to −80 mV and whole cell series resistance (<8.5 MΩ) was compensated for by 95% with a lag of 9 μs. Membrane potentials were corrected online for a liquid junction potential of −11 mV.

Electrical stimulation at the midline was done as previously described (Lorteije *et al.* 2009). Time course and magnitude of STD was estimated from responses to a 400 ms, 500 Hz stimulus train (five repetitions at intervals of 10 s) and a 1.5 s, 50 Hz train (1–5 repetitions). To study the effect of *in vivo*-like background activity on STD during high frequency firing, a 31 s, 50 Hz stimulus train was applied starting 100 ms after a 400 ms, 500 Hz train. This combined stimulus train was repeated for a minimum of ten times at an inter-train interval of 20 ms. To test for tonic $GABA_B$ receptor activation in basal slice conditions, calyces were stimulated before and after bath application of CGP54626 alone and in combination with baclofen at a stimulus interval of 10 s.

Stimulus trains were generated using a National Instruments board (Austin, TX, USA), triggered using Clampex 8.2 (Axon Instruments, Union City, CA, USA) protocols via a Digidata 1320A 16-bit A/D converter (MDS Analytical Technologies). Data were acquired using an Axopatch 200B amplifier (MDS Analytical Technologies), filtered at 2–10 kHz with a low pass, four-pole Bessel filter, and sampled at 66.67 or 83.33 kHz with a Digidata 1320A. Of the 31 s, 50 Hz stimulus train, only four stimuli at the beginning (immediately following the 500 Hz train) and 10 stimuli at the end of the train were included in the analysis.

Analysis

Analysis was performed using custom procedures written in the NeuroMatic environment (version 2.00, kindly provided by Dr J. Rothman, University College London, London, UK) within Igor Pro 6.2 (WaveMetrics, Lake Oswego, OR, USA).

Excitatory postsynaptic current (EPSC) amplitudes were measured as previously described (Crins *et al.* 2011). In short, after fitting a double exponential to the decay phase of the preceding EPSC, the value of the fit at the time of EPSC peak being measured was taken as baseline. Amplitudes were calculated as the difference between the peak and estimated baseline values.

All *in vivo* recordings reported in this paper showed evidence for the presence of a prespike.

We previously showed that both the amplitude of the extracellularly recorded EPSP (eEPSP) and its rate of rise (eEPSP′) can be used as a measure of strength (Lorteije *et al.* 2009). In almost half of the cells we recorded from, it was hard to delineate the eEPSP from the amplitude of the extracellularly recorded excitatory postsynaptic potential (eAP). We therefore used the maximum rate of rise of eEPSP as a measure for the strength of transmission.

The iontophoretic application of drugs normally lasted 2–7 min. Cells which showed more than 30% run-down or run-up of eAP were excluded from analysis. In the experiments involving iontophoresis, cells exhibiting similar, simultaneous changes in eEPSP′ and eAP during iontophoresis were also excluded from analysis.

Amplitudes were fitted with a simple model for short-term plasticity (Varela *et al.* 1997) as described previously (Crins *et al.* 2011). In its simplest form, a single depression state parameter decreases at each event with a fraction called the 'depletion factor' and recovers continuously back to 1 with a single time constant. Synaptic transmission is equal to the product of the depression state parameter and the transmission strength in the absence of short-term depression. The depletion factor thus provides an estimate for the release probability of vesicles in the readily releasable pool, even though its value is constrained by the stimulation pattern. In slice recordings, we compared the estimate for the release probability of the vesicles in the readily releasable pool obtained with the depletion model to the estimate obtained by the back-extrapolation method (Schneggenburger *et al.* 1999). This estimate is obtained by first plotting the cumulative EPSC amplitudes during a high-frequency train against the stimulus number, followed by a line fit on the steady-state portion of the train. The value of this line at the first stimulus provides an estimate of the total postsynaptic current that can be evoked by the readily releasable pool, and the ratio of the amplitude of the first EPSC and this estimate provides an estimate for the release probability of the vesicles in the readily releasable pool.

Data are presented as the mean ± standard error of the mean (SEM). Statistical significance of differences between means was assessed using Student's *t* test.

Results

We studied the contribution of spontaneous activity and of $GABA_B$ receptors to synaptic transmission in the young-adult calyx of Held synapse in the mouse. Synaptic transmission was studied both *in vivo*, using juxtacellular recordings, and in slices, by making whole-cell voltage clamp recordings. *In vivo* recordings from the principal neurons were readily identified by the presence of a characteristic extracellular waveform (Fig. 1*A*, inset; Guinan & Li, 1990; Lorteije *et al.* 2009). Their spontaneous frequency ranged between 0.8 and 96 Hz; on average it was 31 ± 7 Hz ($n = 21$). A 400 ms noise burst at 80 dB elicited a clear increase in their firing frequency (Fig. 1*B*),

which reached a maximum of 335 ± 12 Hz within the first 10 ms. The average firing frequency during the last 50 ms of the noise burst was 186 ± 10 Hz. Following the noise burst spontaneous activity was briefly suppressed (Sommer *et al.* 1993; Kadner *et al.* 2006). This silent period is probably inherited from the cochlear nucleus as it lacked prespikes, although we cannot exclude a possible contribution for presynaptic spike propagation failures due to increased Na^+/K^+ ATPase activity (Kim & von Gersdorff, 2012). During spontaneous activity, 6 of 21 juxtacellular recordings demonstrated failures (range 1.1–55%), with an average failure rate in all cells of 5.2 ± 3.0%. During auditory stimulation 9 of 21 cells showed failures (range 3.6–37%), but the overall failure rate increased only slightly to 7.7 ± 2.8%.

Cells with low spontaneous activity show relatively large STD during sounds

To test for the presence of short-term plasticity, we quantified the maximum of the first derivative of the extracellularly recorded EPSP (eEPSP′) of the complex waveforms, as described in the Methods. An example of the changes in the average amplitude during the sound stimulation is shown in Fig. 1*C*. In Fig. 1*D*, the amplitudes are averaged based on the number of preceding events after sound onset. The second eEPSP′ evoked by acoustic stimulation was larger than the first, suggesting the presence of paired pulse facilitation. Later during the noise burst, the average eEPSP′ size decreased, and became smaller than the average spontaneous amplitude, suggesting that the prolonged high-frequency stimulation induced STD. In Fig. 1*E* the eEPSP′ is displayed as a function of the interval with its preceding event, again illustrating that at short intervals the average eEPSP′ is somewhat smaller.

The cell illustrated in Fig. 1 had a relatively low spontaneous frequency of only 9 Hz. We observed that cells with a low spontaneous frequency often had clear evidence for the presence of STD, whereas cells with a spontaneous frequency >20 Hz generally showed little or no STD. An example of a cell with a relatively high spontaneous firing frequency of 53 Hz is shown in Fig. 2. In this cell the average eEPSP′ showed only a small decrease during the noise burst, whereas the firing frequency reached during the noise burst (Fig. 2*C*) was similar as in the cell displayed in Fig. 1. There was also no evidence for the presence

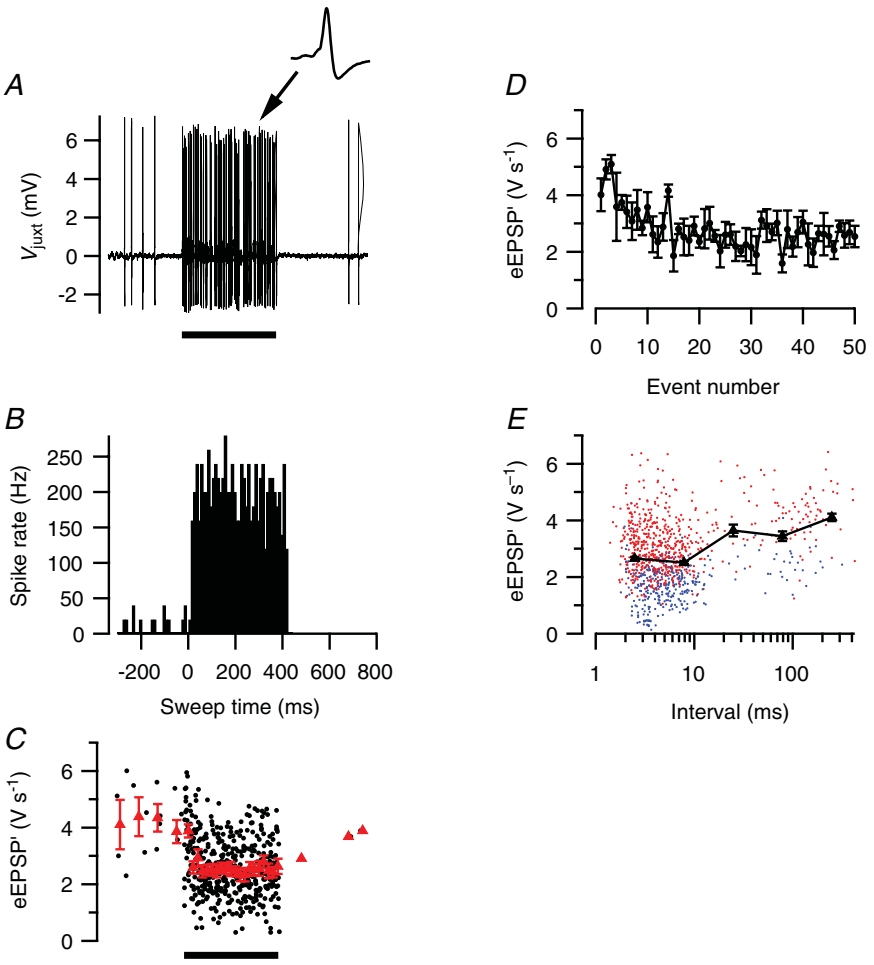

Figure 1. Sound-induced short-term plasticity in a cell with low spontaneous activity
A, *in vivo* juxtacellular recording from a principal neuron in the MNTB showing a large increase in activity during 400 ms, 80 dB noise burst (solid bar), followed by a period of reduced activity. Inset shows an example of a characteristic complex waveform. *B*, peristimulus time histogram (PSTH) of sound-evoked activity. Histogram is based on five sound presentations. *C*, reduction of the maximum rate of rise of the extracellular EPSP (eEPSP′) during sound stimulation. Red triangles indicate binned averages. *D*, event amplitude as a function of the event number evoked by the sound. *E*, relationship between event amplitudes and preceding interval. Triangles indicate log-binned averages. Blue and red symbols indicate subthreshold and suprathreshold events, respectively. All data are from the same cell.

of synaptic facilitation, as the second EPSP evoked by acoustic stimulation had a similar size as the first EPSP.

On average the eEPSP′ amplitude decreased to 82 ± 3% of control ($n = 21$ cells). An overview of the relationship between the eEPSP′ amplitude towards the end of the sound and the spontaneous frequency showed that cells with a spontaneous frequency >20 Hz showed little depression (92 ± 2% of control, $n = 11$), whereas cells with a lower spontaneous frequency on average showed much more depression (71 ± 4% of control, $n = 10$; Fig. 3). In the 12 recordings that did show a clear inflection between the eEPSP and the eAP (e.g. inset to Fig. 2*A*), measurements of eEPSP amplitudes and maximum slopes (eEPSP′) yielded similar amounts of depression during the noise bursts ($P = 0.23$, paired t test). It seems unlikely that the observed inverse relationship between spontaneous firing frequency and steady-state depression was due to a difference in firing rates during auditory stimulation. There was no obvious correlation between average firing rate during the last 50 ms of the noise burst and the spontaneous firing frequency ($r = 0.15$, $P = 0.52$). Even though the data did show an inverse relationship between the amount of depression and the maximum firing rate ($r = -0.41$), this did not reach significance ($P = 0.06$), in contrast to the relationship between spontaneous firing rate and depression ($r = -0.65$, $P = 0.002$). There was a significant inverse relationship between the maximum firing rate during the noise burst and the spontaneous frequency ($r = -0.46$, $P = 0.036$), and after controlling for the effect of spontaneous activity, the correlation between maximum evoked frequency and steady-state depression was strongly reduced (partial correlation $r = -0.19$, $P = 0.44$). In addition, the steady-state depression levels were reached well after the peak of the peristimulus time histogram (PSTH), suggesting that the spontaneous activity affected both the maximum attained frequency and the steady-state depression, but that differences in the maximum frequency were not responsible for the observed relationship between spontaneous frequency and steady-state depression.

To allow a comparison between the cells, which all had a different spontaneous firing frequency, we fitted the firing patterns with a simple model for short-term plasticity (Varela *et al.* 1997). Only 7 of 21 cells showed clear facilitation at the beginning of acoustic stimulation (e.g. Fig. 1*D*). To simplify the comparison further, we therefore neglected short-term synaptic facilitation. Despite the simplicity of the model, it matched the average steady-state depression well ($r = 0.94$). An example is shown in Fig. 4*A*. The depletion factor obtained from the fit with the simple depletion model provides an estimate for the release probability of vesicles in the readily releasable pool. On average, neurons with a spontaneous frequency of <20 Hz had a depletion factor of 0.024 ± 0.005 and a recovery time constant of 200 ± 60 ms, with 22 ± 3% of

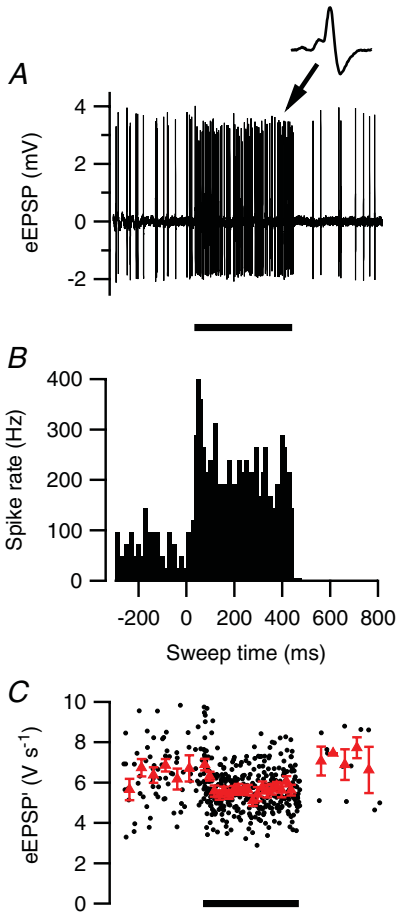

Figure 2. Little short-term plasticity in a cell with high spontaneous activity
A, *in vivo* juxtacellular recording from a principal neuron in the MNTB showing both high spontaneous activity and evoked response during 400 ms, 80 dB noise burst. Inset shows an example of a characteristic complex waveform. *B*, peristimulus time histogram (PSTH) of sound-evoked activity. *C*, mild reduction of the maximum rate of rise of the extracellular EPSP (eEPSP′) during sound stimulation. Triangles indicate binned averages. Error bars indicate SEM. *B* and *C* are based on five sound presentations.

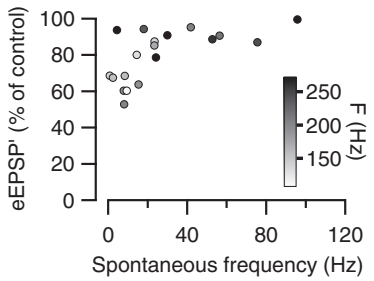

Figure 3. Relationship between eEPSP′ and spontaneous firing frequency
Event amplitudes were averaged during the last 50 ms of the sound, and are shown as a percentage of the average amplitude during the 200 ms preceding the sounds. The symbol filling indicates the average firing frequency during the last 50 ms of the sound.

the variance in the amplitude explained by the model, whereas the neurons with a spontaneous frequency of >20 Hz had a depletion factor of only 0.010 ± 0.003 and a recovery time constant of 185 ± 52 ms, with 10 ± 2% of the variance explained (Fig. 4*B* and *C*). The combination of larger depletion factor and similar recovery time constant in cells with low spontaneous activity predicts a larger sound-evoked depression than in cells with high spontaneous activity.

The effect of spontaneous frequency on STD in slice experiments

An obvious explanation for the results shown in Fig. 2 is that higher spontaneous frequencies lead to larger, tonic depression of the synapse, resulting in reduced additional depression during the sound stimulation. The alternative interpretation, however, is that the calyces with higher spontaneous frequencies have intrinsically different properties from calyces with low spontaneous frequencies, making them more resistant to synaptic depression. The latter possibility is supported by the observation that the amount of steady-state depression during the sound stimulation in the neurons with low spontaneous firing frequency was quite variable, whereas this variability was not caused by differences in the firing rates during the sound stimulation (Fig. 3). To discriminate between these two explanations we attempted to reduce the spontaneous firing frequency by cooling the cochlea, but this unfortunately also strongly affected evoked activity (T. Wang, unpublished results). We therefore tested the effect of spontaneous firing in a slice experiment, which allowed us to test the amount of STD evoked by a high-frequency train in the presence and absence of spontaneous activity within the same cell. The extracellular calcium concentration in these experiments was 1.2 mM, which is on the low range of *in vivo* estimates (Borst, 2010). An example of the response to a 400 ms, 500 Hz train is shown in Fig. 5*A*. In response to the tetanus, the EPSC amplitude depressed from an initial value of −4.8 nA to a steady-state value of −3.1 nA. A continuous 50 Hz stimulus already depressed the EPSCs to a value of −3.2 nA (Fig. 5*B*). During the 500 Hz tetanus, the EPSC further declined to a value of −2.1 nA. Following the train, an overshoot in the EPSC amplitudes was observed, which may be a reflection of post-tetanic potentiation (Habets & Borst, 2005; Korogod *et al.* 2005). Because the EPSC at the start of the 500 Hz train was smaller in the presence of the 50 Hz stimulation, the relative decline during this 500 Hz train was smaller as well. Similar results were obtained in six other experiments (Fig. 5*E*, *F* and *I*). On average, the EPSC depressed to 43 ± 6% of the first EPSC in the 500 Hz train in the absence and to 70 ± 5% in the presence of the 50 Hz conditioning train ($P < 0.001$, paired t test; Fig. 5*I*). Steady-state levels at the end of the 500 Hz train were similar in both types of experiments (−2.1 ± 0.3 and −1.9 ± 0.3 nA, respectively; Fig. 5*E* and *F*). To allow a comparison with the *in vivo* experiments, we fitted the EPSC amplitudes with the simple depletion model. Recordings with and without the conditioning train were fitted separately, to test the impact of spontaneous firing on the depletion factor. In the experiments with a conditioning train, the start of the conditioning train was not used, to allow a better comparison with the *in vivo* data where spontaneous activity was continuously present. The quality of the fits was confirmed by comparing the measured and the fit-predicted steady-state depression and the recovery time constants from depression (data not shown). The depletion factor decreased from 0.067 ± 0.009 to

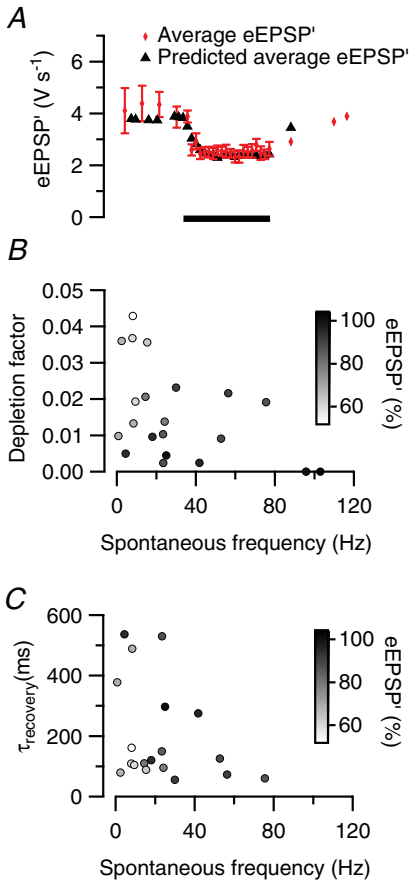

Figure 4. Fit of event amplitudes with a short-term plasticity model
A, predicted reduction of the maximum rate of rise of the extracellular EPSP (eEPSP′) during sound stimulation by a fit with a simple depletion model (depletion factor 0.036, recovery time constant 89 ms). Black triangles indicate the predicted eEPSP′; red diamonds indicate binned averages of measured eEPSP′. *B*, relationship between depletion factor obtained from fits and spontaneous firing frequency. Symbol filling indicates relative eEPSP′ size during the last 50 ms of the sound presentation. *C*, relationship between recovery time constant obtained from fits and spontaneous frequency. Symbol filling as in *B*.

0.026 ± 0.005 ($n = 6$) in the presence of the conditioning train. The apparent recovery time constant was larger in the presence of the conditioning train (147 ± 39 ms, $n = 6$) than with the 500 Hz train only (57 ± 3 ms). The results of these fits indicate that the spontaneous firing activity can contribute to the differences in short-term plasticity during sound stimulation.

A common alternative way to estimate the release probability of the vesicles in the readily releasable pool is by plotting the cumulative amplitudes of EPSCs during a high-frequency train against time and making a line fit on the steady-state part (Fig. 5*J*). The back-extrapolation of the line to the start of the train provides an estimate for the total postsynaptic current that can be elicited by the readily releasable pool and the relative size of the first EPSC provides an estimate of the release probability (Schneggenburger *et al.* 1999). The estimated release probability was about twice as high as the estimate obtained with the fit with the depletion model (0.131 ± 0.015 *vs.* 0.067 ± 0.009). The difference was not caused by a bad fit with the depletion model, as the measured data and fit estimates generally overlaid well (Fig. 5*J*). Additionally, the back-extrapolation method applied to the amplitudes predicted by the results of the

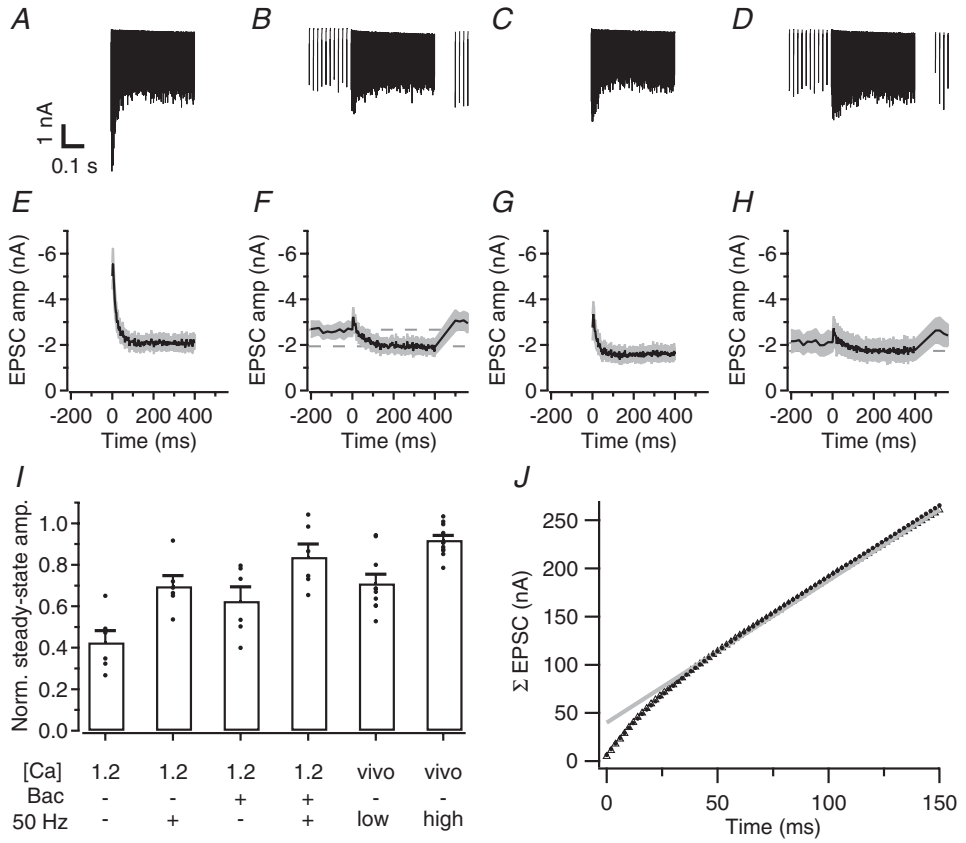

Figure 5. Modulation of STD by baclofen and *in vivo*-like activity in slices
A, sample traces of EPSCs from one cell, evoked at 500 Hz in aCSF containing 1.2 mM calcium. *B*, sample traces recorded in the same cell as in *A* during application of the 500 Hz train followed 100 ms later by a 31 s, 50 Hz train. Trace shows an average of the last 5 of 16 repetitions of the stimulus. *C*, *D* as in *A*, *B*, respectively, except the aCSF contained 100 μM baclofen. *E*, average EPSCs amplitudes from six cells, measured during a 500 Hz stimulus train at 1.2 mM Ca^{2+}. Grey area denotes standard error. *F*, as in *E*, except the combined 500 Hz and 50 Hz train was applied. *G*, *H* as in *E*, *F*, respectively, except the aCSF contained 100 μM baclofen. The stimulus was repeated at least 10 times per experiment and the last five repetitions were averaged for each of the six recorded cells. *I*, summary of steady-state amplitudes measured for each experimental condition, calculated as the average of the last 10 EPSCs of the high-frequency train and normalized to the respective first EPSCs. Only cells where all experimental conditions were applied are included. Filled circles represent individual cells; bars represent averages across cells ± SEM. *J*, estimate of the release probability of the readily releasable pool. Open triangles show the relationship between the cumulative amplitudes of the averaged EPSCs shown in *A* and the time during the 500 Hz train. Grey continuous line shows the line fit of the cumulative EPSCs starting at 100 ms. The back-extrapolated value at $t = 0$ provides an estimate for the size of the readily releasable pool, which in this case was 39.8 nA. The ratio of the first EPSC and this pool size provides an estimate of the release probability, which was in this case 0.12. Also shown are the fit predictions for the cumulative EPSC amplitudes (solid circles) which overlay well with the measured EPSCs.

fit with the depletion model resulted in similar values for the readily releasable pool size as the measured ones (40.4 ± 6.5 *vs.* 40.2 ± 5.7 nA) and also in much higher values for the apparent release probability (0.147 ± 0.010) than the fitted depletion factors.

Together, the effect of spontaneous frequency in slices and in the *in vivo* experiments strongly suggests that spontaneous firing can tonically depress the calyx of Held synapse and that this effect is stronger for frequencies above 20 Hz than below. This conclusion is in agreement with previous slice work in the calyx synapse (Hermann *et al.* 2007, 2009; Lorteije *et al.* 2009).

Baclofen reduces STD in slice recordings

The amount of depression during the sound stimulation was about 20% on average, which is much smaller than in most slice experiments (reviewed in Borst & Soria van Hoeve, 2012), including the experiments illustrated in Fig. 5*A*. Apart from developmental factors (Crins *et al.* 2011; Sonntag *et al.* 2011) and differences in the extracellular calcium concentration (Lorteije *et al.* 2009), neither of which should contribute in the present experiments, and the spontaneous activity discussed above, another possible regulator of the release probability of the calyx of Held is the GABA$_B$ receptor. We therefore tested to what extent synaptic transmission can be inhibited by GABA acting via presynaptic GABA$_B$ receptors in the young-adult calyx of Held. By reducing release probability, activation of the presynaptic GABA$_B$ receptor may reduce STD as well. In the juvenile synapse, GABA$_B$ receptors can strongly inhibit transmitter release (Isaacson, 1998; Takahashi *et al.* 1998; Kajikawa *et al.* 2001; Sakaba & Neher, 2003). To test whether this is also the case in the young-adult synapse, we studied the effect of the GABA$_B$ receptor agonist baclofen on EPSCs in slices. Baclofen (100 μM) reduced the EPSCs at the start of the 500 Hz train from -5.0 ± 0.6 to -2.8 ± 0.6 nA ($n = 6$, $P = 0.02$; Fig. 5*G*). In the presence of baclofen, the 400 ms, 500 Hz tetanus reduced the EPSCs to only 62 ± 7% of the amplitude of the first EPSC, a significantly smaller depression than in the absence of baclofen ($P = 0.02$; Fig. 5*G* and *I*). In the presence of baclofen and the 50 Hz background activity, the 500 Hz tetanus reduced the EPSCs to only 84 ± 6%, which was a significantly smaller reduction than in the absence of baclofen ($n = 6$, $P = 0.02$; Fig. 5*H* and *I*).

Estimating drug concentrations during *in vivo* iontophoresis

We next examined the effect of baclofen under *in vivo* conditions. During initial experiments the drug was applied at the brain surface using a perfusion system. Although baclofen did reduce transmission, quantification was not straightforward, as the onset of the effect was uncertain owing to the diffusional delay in combination with the limited stability of the recordings. We therefore applied the antagonist in the immediate vicinity of the synapse using piggyback electrodes (Havey & Caspary, 1980), as detailed in the Methods. In these experiments we performed two types of controls.

To allow iontophoresis, baclofen had to be applied in an acidic solution (pH 3). As low pH can inhibit synaptic transmission (Chesler, 2003), we tested the effect of the solution in which the baclofen was applied. At high ejection currents the pH 3 solution could fully block transmission, while the prespikes remained intact, indicating that the low pH did not block presynaptic action potentials (data not shown). Low pH solution also did not induce any obvious effect on the extracellularly recorded postsynaptic action potential. The effect of low pH on synaptic transmission was rapidly reversible. An example of a small blocking effect observed at an ejection current of 300 nA is shown in Fig. 6*A*. In this experiment we therefore lowered the ejection current to 200 nA, thus minimizing the inhibitory pH effect.

A second control that we performed was to apply a solution containing the calcium buffer EGTA to get a better estimate of the concentration reached within the synaptic cleft by the applied drugs. By reducing the extracellular calcium concentration, EGTA will reduce transmitter release. An example is shown in Fig. 6*B*. This example shows that the blocking effect continues to increase throughout the application, presumably as a result of accumulation of EGTA in the synaptic cleft. Similar effects were observed in six experiments. In Fig. 6*B*, EGTA was applied for 5 min at -200 nA. In the first 3 min, the duration that was used to apply baclofen in the same cell (Fig. 6*C*), EGTA reduced the eEPSP′ to 45% of control and substantially increased the percentage of failures. Assuming that the dependence of transmitter release on the extracellular Ca^{2+} concentration follows a power law with an exponent of 2.5 (Barnes-Davies & Forsythe, 1995; Wu *et al.* 1998; Schneggenburger *et al.* 1999; Fedchyshyn & Wang, 2005), the estimated reduction in the extracellular calcium concentration would be about 25%, or 0.3 mM at a (low) estimate of 1.2 mM for the interstitial Ca^{2+} concentration. As the current was entirely carried by EGTA, which was present in the pipette at a concentration of 160 mM, the EGTA was diluted approximately 500-fold compared to the pipette concentration. In the other cells, using ejection currents ranging from -150 to -400 nA, on average the eEPSP′ was reduced to 43 ± 6% ($n = 9$) of control, translating to an average dilution of about 500-fold (range 300–1200×).

Inhibition of *in vivo* transmission by baclofen

The effect of iontophoretic application of baclofen on *in vivo* synaptic transmission in the MNTB is shown in Fig. 6*C*. Within 30 sec after the start of the application the amplitudes started to decrease, reaching a new steady-state value after about 2 min. Under the assumption that baclofen is ejected equally efficiently as the other ions in the pipette and diffuses similarly to EGTA, ejecting baclofen at the same current level for the same amount of time would result in a similar dilution as in the EGTA experiments discussed above, suggesting that baclofen concentrations reached in the synaptic cleft were about 20 μM. As the EGTA experiments indicated that its concentration continued to increase at the synapse throughout its application, the presence of a plateau suggested that baclofen was present in a saturating concentration. After the ejection stopped, the blocking effect reversed in about 3 min. On average, baclofen reduced the spontaneous eEPSP′ to 61 ± 9% of control ($n = 6$ cells), similar to what was observed in the slice experiments. The onset of the block could generally be well described by an exponential function, with an average time constant of 86 ± 21 s. On average, baclofen application significantly increased the spontaneous failure rate from 10 ± 7 to 43 ± 11% ($P = 0.03$, paired t test), and increased the sound-evoked failure rate from 12 ± 6 to 36 ± 8% ($P = 0.04$). The difference in baclofen-evoked failure rate in the presence or absence of sound stimuli was not significant ($P = 0.6$, paired t test). No obvious changes were observed in the postsynaptic action potential waveform in the presence of baclofen, suggesting that the main effect of baclofen was presynaptic.

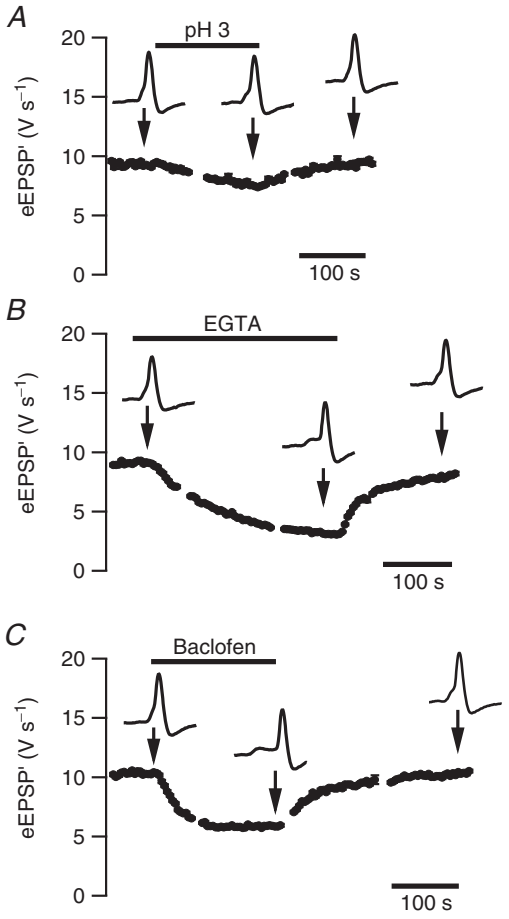

Figure 6. Changes in synaptic transmission during *in vivo* iontophoresis
A, a 155 s, −300 nA application of saline solution of pH 3 resulted in a small, reversible reduction in event amplitudes. *B*, a 300 s, −200 nA application of EGTA (160 mM) gave a strong, reversible reduction in event amplitudes. *C*, reversible, inhibitory effect of iontophoretic application of baclofen (10 mM; 185 s, −200 nA). All data are from the same cell. Error bars are only shown if SEM is larger than symbol size.

Baclofen reduces STD *in vivo*

By changing release probability, baclofen would be expected to change short-term plasticity induced by the sound stimulation. On average, baclofen increased the paired-pulse facilitation of sound-evoked eEPSP′ and decreased STD (Fig. 7). Paired-pulse facilitation at sound onset increased from 1.27 ± 0.09 to 1.42 ± 0.06 ($n = 6$, $P = 0.047$) and steady-state amplitudes during the last 50 ms of the noise burst from 75 ± 6% of the amplitude of spontaneous events in the absence of baclofen to 89 ± 6% of the amplitude of spontaneous events in the presence of baclofen ($P = 0.12$). These results suggest that $GABA_B$ receptors regulate STD at the calyx of Held synapse *in vivo* by reducing the release probability of vesicles in the readily releasable pool.

Low ambient GABA concentration both in slices and *in vivo*

We next investigated whether the presynaptic $GABA_B$ receptor is tonically activated by ambient GABA in slices and *in vivo*. EPSC amplitudes were not affected by the high affinity $GABA_B$ receptor antagonist CGP54626 (10 μM) in slices (103 ± 13% of control; Fig. 8). The effectiveness of CGP54626 at the calyceal $GABA_B$ receptors was confirmed by its ability to block the inhibitory effects of baclofen (100 μM) on EPSC amplitudes (110 ± 15%, $n = 6$). We conclude that the extracellular GABA concentration during slice recordings is too low to activate $GABA_B$ receptors on the calyx of Held significantly.

To test whether the presynaptic $GABA_B$ receptors of the calyx of Held are tonically activated *in vivo*, we initially applied CGP54626 to the brain surface, using a local perfusion system. Even at concentrations as high as 1 mM, it did not affect the eEPSP′ amplitudes ($n = 6$

cells from six different animals; data not shown). We confirmed in each case that the calyx of Held synapse we recorded from, which was typically located at a depth of 400–600 μm, could be reached by substances applied at the surface by applying a solution containing EGTA (20 mM) to the surface. This solution inhibited transmission with a typical time course of 80–120 s. An unfortunate limitation of these experiments, however, is that CGP54626 is a lipophilic drug. Despite the positive EGTA control, it could not be ascertained that it did reach the synapse we recorded from. We therefore used the piggyback method to apply CGP54626 more locally. We did not observe a significant effect on synaptic transmission upon the iontophoretic application of CGP54626 (Fig. 9*A*). On average the eEPSP′ amplitude showed a slight, non-significant decrease of $-4 \pm 4\%$ ($n = 6$, $P = 0.34$) during CGP54626 application. In these experiments CGP54626 was applied using similar ejection currents (200–500 nA) for a similar period (1–3 min) as used in the *in vivo* baclofen experiments described above. In these experiments two barrels containing EGTA and pH 3 solution again served as controls. To further confirm that CGP54626 did reach the recorded synapse, we also applied CGP54626 along with baclofen. The effect of the combined drugs was similar as with CGP54626 alone ($-4 \pm 3\%$, $n = 5$, $P = 0.4$; Fig. 9*B*), indicating that CGP54626 did reach the synaptic cleft and was able to block the action of baclofen. In addition, there was no difference in STD during the iontophoretic application of both drugs (data not shown). Taken together, these results indicate that both in slices and *in vivo* the ambient GABA concentration is not high enough to activate the presynaptic GABA$_B$ receptor measurably.

Discussion

We tested the effect of spontaneous activity and of GABA$_B$ receptor activation on the release probability of the young-adult mouse calyx of Held synapse. We found clear evidence that the calyx of Held synapse can be tonically depressed by spontaneous activity. We show that activation of the presynaptic GABA$_B$ receptor can further reduce release probability and thus reduce short-term depression, but that the ambient GABA concentration in the MNTB

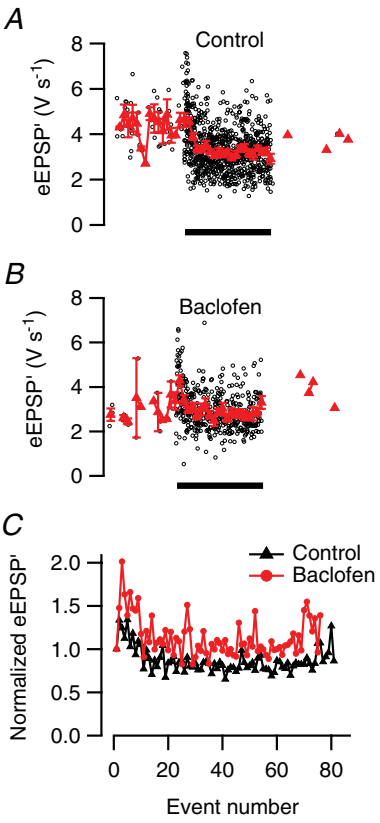

Figure 7. Reduction of STD by activation of GABA$_B$ receptors
A, sound presentation (filled bar) induces clear STD of the synaptic transmission in the absence of baclofen. *B*, during iontophoretic baclofen application, STD is reduced and responses facilitate at sound onset. *A* and *B* are based on six sound presentations. *C*, overlay of normalized event amplitudes during the noise burst in the presence and absence of baclofen.

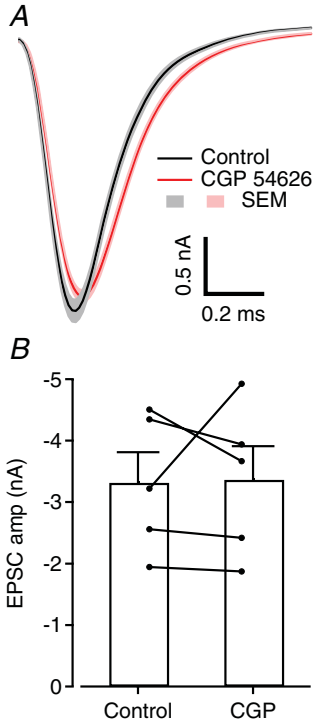

Figure 8. Low ambient GABA concentration in slices of the auditory brainstem
A, average EPSCs recorded from one cell in control conditions (black) and in the presence of 10 μM CGP54626 (red); light colours represent ± SEM. *B*, bar chart showing average EPSC amplitude measured in five cells before and after perfusion of CGP. Filled circles are cell averages and error bars represent SEM.

is too low to activate the presynaptic $GABA_B$ receptor significantly.

Estimating the concentration of drugs during *in vivo* microiontophoresis

To test the function of $GABA_B$ receptors *in vivo*, we adapted the piggyback recording method (Havey & Caspary, 1980) to combine juxtacellular (loose patch) recordings with multibarrel microiontophoresis. We previously showed that juxtacellular recordings of the calyx of Held synapse can be used to estimate both release and postsynaptic excitability (Lorteije *et al.* 2009). By including controls that allowed a better estimate of the drug concentrations at the synapse, we further reduce the gap between the technical possibilities that slice recordings allow and the *in vivo* recordings. We used two types of controls. A pH control was important in our hands, as too high ejection currents led to a block of synaptic transmission with both rapid onset and rapid reversal. It is well known that extracellular acidosis can depress neuronal excitability, among others by modulating ion channels, including voltage-dependent ion channels, ligand-gated ion channels and proton-gated ion channels (reviewed in Chesler, 2003). Its inhibitory effect on voltage-dependent Ca channels (Tombaugh & Somjen, 1996) could account for the strong effects on release. Release in the young-adult calyx of Held is entirely controlled by Cav2.1 (P/Q) channels (Iwasaki *et al.* 2000), which show both lower conductance and a positive shift in activation at low pH (Cens *et al.* 2011). The other control we used was to apply a solution containing the calcium buffer EGTA. EGTA has a dissociation constant (K_d) $<1\ \mu$M (Portzehl *et al.* 1964), indicating that under our recording conditions virtually all ejected EGTA will bind extracellular calcium. The high sensitivity of transmitter release to changes in extracellular calcium allows an estimate of the concentration of EGTA that is reached in the synaptic cleft. Although this method substantially increases the accuracy of the estimates of the concentration reached in these experiments, they still depend on a number of uncertainties, including the exact dependence of transmission on the extracellular calcium concentration, for which previous slice experiments have estimated 2nd to 3rd power relationships (Barnes-Davies & Forsythe, 1995; Fedchyshyn & Wang, 2005), and the estimates of the transport number (Hicks, 1984) of EGTA and drugs.

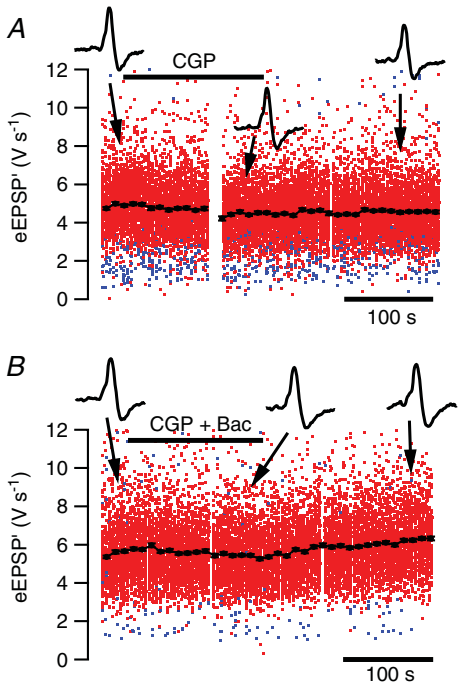

Figure 9. Low ambient GABA concentration in the auditory brainstem *in vivo*
A, lack of effect of 160 s, –200 nA application of the $GABA_B$ antagonist CGP54626 (1 mM; filled bar) on synaptic transmission. Insets show representative extracellular waveforms at the times indicated by the arrows. Red dots are suprathreshold events, blue subthreshold. Filled circles indicate time-binned averages; error bars are typically smaller than the symbol size. *B*, in the presence of CGP54626, application of baclofen (10 mM; 150 s, −200 nA; filled bar) in the same cell did not reduce synaptic transmission.

Low ambient GABA concentration in the MNTB

We used a pharmacological approach to test the contribution of the $GABA_B$ receptor of the calyx of Held to release probability. Previous slice studies had shown that in many regions of the brain, the $GABA_B$ receptor is tonically activated by ambient GABA (Emri *et al.* 1996; Kombian *et al.* 1996; Le Feuvre *et al.* 1997; Lin & Dun, 1998; Aroniadou-Anderjaska *et al.* 2000; Kirmse & Kirischuk, 2006; Wu *et al.* 2011). This question has received less attention in *in vivo* studies (but see Pírez & Wachowiak, 2008), presumably because of the difficulties in separating presynaptic from postsynaptic or network effects in most regions. The piggyback recordings of the calyx of Held synapse allowed us to test this question *in vivo*. The simple input–output relation within the MNTB makes a contribution of network and postsynaptic effects highly unlikely, whereas the multibarrel approach allowed performing controls to confirm that the $GABA_B$ receptor antagonist did reach the presynaptic receptors. We found both in slices and *in vivo* that application of the $GABA_B$ receptor antagonist CGP54626 did not increase synaptic transmission, indicating both *in vivo* and under slice conditions that the ambient GABA concentration in the MNTB is too low to activate this receptor significantly. It seems unlikely that the concentrations of CGP54626 were too low. At a concentration as low as 1–2 μM, it already completely inhibits the effects of 50–100 μM

baclofen on both pre- and postsynaptic GABA$_B$ receptors at mossy fibre–CA3 pyramidal neuron synapses (Guetg *et al.* 2009), whereas much higher concentrations were reached in the present experiments and GABA has a lower affinity for the GABA$_B$ receptor than baclofen. It is also unlikely that the CGP54626 was unable to prevent the action of GABA, as CGP54626 has been shown to act as an inverse agonist on the GABA$_B$ receptor in experiments in which it attenuated basal signalling of a constitutively active GABA$_B$ receptor (Mukherjee *et al.* 2006), and CGP54626 was able to prevent the inhibitory action of baclofen both *in vivo* and *in vitro* in our control experiments. We cannot exclude that other presynaptic metabotropic receptors for adenosine, glutamate, noradrenaline or serotonin do have tonic effects, although their impact on release is much smaller than that of GABA in mature calyces (Elezgarai *et al.* 1999; Leão & von Gersdorff, 2002; Kimura *et al.* 2003; Renden *et al.* 2005; Mizutani *et al.* 2006).

Typical ambient GABA concentrations in the CNS have been estimated to range between 0.1 and 0.8 μM (Lerma *et al.* 1986; Tossman *et al.* 1986; Dvorzhak *et al.* 2010). The predicted ambient GABA concentration depends on the density of GABA transporters (Roth & Draguhn, 2012). In the MNTB, GABA transporters have yet to be identified, although GAT3 appears to be the prevalent isoform expressed in the brainstem (Clark *et al.* 1992; Durkin *et al.* 1995; Höfner & Wanner, 2004). This isoform is abundant in glial cells where it is primarily located on distal astroglial processes (Minelli *et al.* 1996; Ribak *et al.* 1996). The calyx of Held is surrounded by astroglial processes, which have been suggested to play a role in maintaining low basal levels of neurotransmitters (Sätzler *et al.* 2002; Renden *et al.* 2005; Ford *et al.* 2009). Apart from immunocytochemical studies, experiments showing a stronger tonic GABAergic presynaptic inhibition in the presence of GABA uptake inhibitors would be needed to support an astroglial involvement in regulating the extracellular GABA concentration (Lei & McBain, 2003).

The predicted ambient GABA concentration will not only depend on the presence of GABA transporters, but also on intra-/extracellular Cl^- and Na^+ gradients and on the intracellular GABA concentration (Attwell *et al.* 1993). The intracellular chloride concentration is low in the adult superior olivary complex (Löhrke *et al.* 2005). The intracellular GABA concentrations within the MNTB are not known exactly, but are not expected to be very high in the principal neurons of the MNTB (Hassfurth *et al.* 2010). These observations are thus also compatible with the idea that the ambient GABA concentration in the MNTB is too low to tonically activate the GABA$_B$ receptors on the calyx of Held, which have an affinity for GABA of about 10 μM (Takahashi *et al.* 1998). An earlier slice study also did not observe evidence for tonic activation of GABA$_B$ receptors on terminals innervating bushy cells of the anteroventral cochlear nucleus (AVCN; Lim *et al.* 2000), which are the cells that form the calyx of Held.

Function of GABA$_B$ receptor in the young-adult mouse calyx of Held

We observed that high concentrations of the GABA$_B$ receptor agonist baclofen approximately halved the strength of synaptic transmission at the young-adult calyx of Held synapse, both *in vivo* and in slices. In previous studies in rats, which were done up to P19, larger effects were observed (Isaacson, 1998; Takahashi *et al.* 1998; Kajikawa *et al.* 2001; Sakaba & Neher, 2003). The lower impact observed in the present study might be caused by a developmental decrease in GABA$_B$ receptor expression (Malitschek *et al.* 1998; Fritschy *et al.* 1999), which would be in agreement with the developmental decrease observed for the impact of other presynaptic metabotropic receptors at the calyx of Held (Elezgarai *et al.* 1999; Leão & von Gersdorff, 2002; Kimura *et al.* 2003; Renden *et al.* 2005; Mizutani *et al.* 2006). A developmental decrease has also been observed for the impact of presynaptic GABA$_B$ receptors at other projections within the auditory brainstem (Hassfurth *et al.* 2010). However, a species difference between rats and mice cannot be excluded at present. The relatively small effects of the various presynaptic receptors in the adult calyx of Held are in line with its function as an auditory relay synapse (Borst & Soria van Hoeve, 2012).

Activation of the GABA$_B$ receptor at the calyx of Held is known to reduce release probability of the vesicles in the readily releasable pool, among others by inhibiting calcium channels (Isaacson, 1998; Takahashi *et al.* 1998; Wu *et al.* 1998; Kajikawa *et al.* 2001). After hearing onset, the impact of postsynaptic receptor desensitization to STD becomes very small (Taschenberger *et al.* 2002, 2005; Koike-Tani *et al.* 2008). The reduction in STD we observed both *in vivo* and in slices therefore agrees well with this reduction in release probability.

As the ambient GABA concentration appears to be too low to activate the GABA$_B$ receptor significantly, the most likely physiological activation method would be heterosynaptic depression by spillover from GABAergic terminals that innervate the principal neurons (Moore & Moore, 1987; Adams & Mugnaini, 1990; Lu *et al.* 2008). These inhibitory terminals can have a strong impact on the principal neurons in the rat (Banks & Smith, 1992; Awatramani *et al.* 2004, 2005; Lu *et al.* 2008). Their impact in the mouse principal neurons may be less pronounced (Wu & Kelly, 1991, 1995) and their role *in vivo* remains to be established (Lorteije & Borst, 2011). Alternatively, taurine, which can also be released in the brainstem (Saransaari & Oja, 2006) and which can serve as an agonist at GABA$_B$ receptors (Kontro & Oja, 1990), may activate the GABA$_B$ receptors on the calyx of Held.

Presence of STD *in vivo*

We previously reported a minimal impact for STD in the young-adult rodent calyx of Held synapse *in vivo* (Lorteije *et al.* 2009; Crins *et al.* 2011). Although in some neurons evidence for the presence of STD was found, the overall impact was not very large. Similar results were obtained by others (Sonntag *et al.* 2011). Here we find an average of about 20% depression during a long, loud noise burst. We can identify several reasons for this discrepancy. First, in our developmental study in rats (Crins *et al.* 2011) we studied only spontaneous activity, whereas in the present study STD could be observed only during a prolonged increase in firing rate. Secondly, in our previous study in mice in which we did use auditory stimulation, the spontaneous frequencies were generally much higher (71 ± 11 *vs.* 31 ± 7 Hz; Lorteije *et al.* 2009). In the present study we also found little or no STD at spontaneous frequencies above 20 Hz, which constituted the large majority of cells in our previous study. A difference with previous experiments was that here we ventilated the animals, probably resulting in better oxygenation. As a result, basal release probability was probably somewhat higher, as suggested by the shape of the complex extracellular waveform, which showed less inflection between the EPSP and the AP. Another indication that release probability was higher on average was that the fraction of subthreshold EPSPs was somewhat smaller than in our previous studies. The low failure rate is in agreement with the view of the calyx of Held synapse as an auditory relay (reviewed in Borst & Soria van Hoeve, 2012). A low spontaneous frequency can be expected to be more common in cells with a low characteristic frequency (Spirou *et al.* 1990; Kopp-Scheinpflug *et al.* 2008).

Role of spontaneous activity

Our results are in general agreement with earlier studies that have suggested an important role for spontaneous activity in setting the release probability *in vivo* (Hermann *et al.* 2007, 2009; Lorteije *et al.* 2009). Our observation that the amount of STD was on average much larger in cells with low spontaneous frequency than in cells with high spontaneous frequency provides the first *in vivo* evidence for a tonic depression of synaptic transmission at the calyx of Held synapse due to spontaneous activity. An alternative interpretation would be that cells with high spontaneous frequency are more resistant to short-term depression than cells with low spontaneous frequency. Intrinsic differences between calyces with respect to, among others, resistance to depression were recently shown in a study that focused on 2–3 week old mice (Grande & Wang, 2011). Our slice experiments showed that a high spontaneous frequency will reduce the apparent STD induced by high-frequency stimulation. A fit with a simple model for short-term plasticity showed that the depletion factor was about twice as large in the absence as in the presence of spontaneous activity in the same synapse, similar to what was observed *in vivo* for the difference between synapses with low and high spontaneous activity. The depletion factor obtained from these fits provides an estimate for the release probability of vesicles from the readily releasable pool. However, in the absence of measurements of the size of the readily releasable pool, it is hard to assess the relative contribution of pool depletion and decreases in release probability during STD (Wu & Borst, 1999). Moreover, the value obtained for the depletion factor is constrained by the presynaptic firing pattern. Processes with a recovery time much shorter than the shortest interval or much longer than the longest intervals will not contribute to the apparent release probability as obtained from the fits with the depletion model. Despite the simplicity of this model compared to the known heterogeneity of the readily releasable pool in the calyx of Held (Lee *et al.* 2012; Lipstein *et al.* 2013), it could provide a reasonable description of amplitude dynamics in the presence of spontaneous activity. This is in agreement with a study in the gerbil MNTB (Hermann *et al.* 2009), which also found that in the presence of spontaneous activity, a simple first-order resource depletion model provided an acceptable description of the amplitude dynamics. The much more pronounced synaptic depression observed in their experiments may have been due to the higher extracellular calcium concentration and younger animal age.

We compared the depletion factor obtained from the fits with the depletion model with the release probability obtained from the back-extrapolation method (Schneggenburger *et al.* 1999), a commonly used method to estimate the size of the readily release pool and of the release probability of the vesicles therein (reviewed in Schneggenburger *et al.* 2002). In the present experiments the estimate obtained with this method was about twice that from the depletion model fits. The difference lies mostly in the different assumptions for recovery in both methods rather than in poor fit quality, as was evident from the observation that the back-extrapolation method also yielded a relatively high estimate for the release probability when the event amplitudes predicted by the depletion model were used. The back-extrapolation model assumes that recovery rate from depression is constant throughout the train, whereas in the depletion model it is proportional to release. As a result, the estimates for the size of the readily releasable pool are much larger with the latter. This difference is relevant, as it explains part of the discrepancy between slice estimates for the calyx of Held synapse, which were often obtained using the back-extrapolation method and the present *in vivo* estimates, for which the depletion model was used. Still, the depletion factor obtained from the fits was somewhat higher in slices than *in vivo*. Apart

from the higher stimulation frequency applied in slices during the tetanus, other differences could be related to the use of anaesthesia *in vivo* and possible other differences in the composition of the cerebrospinal fluid compared to the solution we used for the slice experiments (reviewed in Borst, 2010). The observed recovery time constant of about 150 ms probably constitutes a weighted average of fast recovery during the train and slower recovery following the trains (Neher & Sakaba, 2008).

In summary, from our experiments we conclude that the difference between *in vivo* and previous slice results can largely be explained by the presence of spontaneous activity and the lower extracellular calcium concentration *in vivo*. Tonic activation of the $GABA_B$ receptor is unlikely to be a major contributing factor to differences between results obtained *in vivo* and in slices.

References

Adams JC & Mugnaini E (1990). Immunocytochemical evidence for inhibitory and disinhibitory circuits in the superior olive. *Hear Res* **49**, 281–298.

Aroniadou-Anderjaska V, Zhou F-M, Priest CA, Ennis M & Shipley MT (2000). Tonic and synaptically evoked presynaptic inhibition of sensory input to the rat olfactory bulb via $GABA_B$ heteroreceptors. *J Neurophysiol* **84**, 1194–1203.

Attwell D, Barbour B & Szatkowski M (1993). Nonvesicular release of neurotransmitter. *Neuron* **11**, 401–407.

Awatramani GB, Turecek R & Trussell LO (2004). Inhibitory control at a synaptic relay. *J Neurosci* **24**, 2643–2647.

Awatramani GB, Turecek R & Trussell LO (2005). Staggered development of GABAergic and glycinergic transmission in the MNTB. *J Neurophysiol* **93**, 819–828.

Banks MI & Smith PH (1992). Intracellular recordings from neurobiotin-labelled cells in brain slices of the rat medial nucleus of the trapezoid body. *J Neurosci* **12**, 2819–2837.

Barnes-Davies M & Forsythe ID (1995). Pre- and postsynaptic glutamate receptors at a giant excitatory synapse in rat auditory brainstem slices. *J Physiol* **488**, 387–406.

Borst JGG (2010). The low synaptic release probability *in vivo*. *Trends Neurosci* **33**, 259–266.

Borst JGG & Soria van Hoeve J (2012). The calyx of Held synapse: from model synapse to auditory relay. *Annu Rev Physiol* **74**, 199–224.

Cens T, Rousset M & Charnet P (2011). Two sets of amino acids of the domain I of Cav2.3 Ca^{2+} channels contribute to their high sensitivity to extracellular protons. *Pflugers Arch* **462**, 303–314.

Chesler M (2003). Regulation and modulation of pH in the brain. *Physiol Rev* **83**, 1183–1221.

Clark JA, Deutch AY, Gallipoli PZ & Amara SG (1992). Functional expression and CNS distribution of a β-alanine-sensitive neuronal GABA transporter. *Neuron* **9**, 337–348.

Crins TTH, Rusu SI, Rodríguez-Contreras A & Borst JGG (2011). Developmental changes in short-term plasticity at the rat calyx of Held synapse. *J Neurosci* **31**, 11706–11717.

Durkin MM, Smith KE, Borden LA, Weinshank RL, Branchek TA & Gustafson EL (1995). Localization of messenger RNAs encoding three GABA transporters in rat brain: an in situ hybridization study. *Brain Res Mol Brain Res* **33**, 7–21.

Dvorzhak A, Myakhar O, Unichenko P, Kirmse K & Kirischuk S (2010). Estimation of ambient GABA levels in layer I of the mouse neonatal cortex in brain slices. *J Physiol* **588**, 2351–2360.

Elezgarai I, Benítez R, Mateos JM, Lázaro E, Osorio A, Azkue JJ, Bilbao A, Lingenhoehl K, Van Der Putten H, Hampson DR, Kuhn R, Knöpfel T & Grandes P (1999). Developmental expression of the group III metabotropic glutamate receptor mGluR4a in the medial nucleus of the trapezoid body of the rat. *J Comp Neurol* **411**, 431–440.

Emri Z, Turner JP & Crunelli V (1996). Tonic activation of presynaptic $GABA_B$ receptors on thalamic sensory afferents. *Neuroscience* **72**, 689–698.

Fedchyshyn MJ & Wang L-Y (2005). Developmental transformation of the release modality at the calyx of Held synapse. *J Neurosci* **25**, 4131–4140.

Ford MC, Grothe B & Klug A (2009). Fenestration of the calyx of Held occurs sequentially along the tonotopic axis, is influenced by afferent activity, and facilitates glutamate clearance. *J Comp Neurol* **514**, 92–106.

Fritschy J-M, Meskenaite V, Weinmann O, Honer M, Benke D & Mohler H (1999). $GABA_B$-receptor splice variants GB1a and GB1b in rat brain: developmental regulation, cellular distribution and extrasynaptic localization. *Eur J Neurosci* **11**, 761–768.

Grande G & Wang L-Y (2011). Morphological and functional continuum underlying heterogeneity in the spiking fidelity at the calyx of Held synapse *in vitro*. *J Neurosci* **31**, 13386–13399.

Grothe B & Koch U (2011). Dynamics of binaural processing in the mammalian sound localization pathway–the role of $GABA_B$ receptors. *Hear Res* **279**, 43–50.

Guetg N, Seddik R, Vigot R, Turecek R, Gassmann M, Vogt KE, Bräuner-Osborne H, Shigemoto R, Kretz O, Frotscher M, Kulik A & Bettler B (2009). The $GABA_{B1a}$ isoform mediates heterosynaptic depression at hippocampal mossy fibre synapses. *J Neurosci* **29**, 1414–1423.

Guinan JJ, Jr. & Li RY-S (1990). Signal processing in brainstem auditory neurons which receive giant endings (calyces of Held) in the medial nucleus of the trapezoid body of the cat. *Hear Res* **49**, 321–334.

Habets RLP & Borst JGG (2005). Post-tetanic potentiation in the rat calyx of Held synapse. *J Physiol* **564**, 173–187.

Hájos N & Mody I (2009). Establishing a physiological environment for visualized *in vitro* brain slice recordings by increasing oxygen supply and modifying aCSF content. *J Neurosci Methods* **183**, 107–113.

Hassfurth B, Grothe B & Koch U (2010). The mammalian interaural time difference detection circuit is differentially controlled by $GABA_B$ receptors during development. *J Neurosci* **30**, 9715–9727.

Havey DC & Caspary DM (1980). A simple technique for constructing 'piggy-back' multibarrel microelectrodes. *Electroencephalogr Clin Neurophysiol* **48**, 249–251.

Hermann J, Grothe B & Klug A (2009). Modeling short-term synaptic plasticity at the calyx of Held using *in vivo*-like stimulation patterns. *J Neurophysiol* **101**, 20–30.

Hermann J, Pecka M, von Gersdorff H, Grothe B & Klug A (2007). Synaptic transmission at the calyx of Held under *in vivo*-like activity levels. *J Neurophysiol* **98**, 807–820.

Hicks TP (1984). The history and development of microiontophoresis in experimental neurobiology. *Prog Neurobiol* **22**, 185–240.

Höfner G & Wanner KT (2004). Evaluation of GABA uptake in subcellular fractions of bovine frontal cortex and brainstem. *Neurosci Lett* **364**, 53–57.

Isaacson JS (1998). $GABA_B$ receptor-mediated modulation of presynaptic currents and excitatory transmission at a fast central synapse. *J Neurophysiol* **80**, 1571–1576.

Iwasaki S, Momiyama A, Uchitel OD & Takahashi T (2000). Developmental changes in calcium channel types mediating central synaptic transmission. *J Neurosci* **20**, 59–65.

Iwasaki S & Takahashi T (2001). Developmental regulation of transmitter release at the calyx of Held in rat auditory brainstem. *J Physiol* **534**, 861–871.

Kadner A, Kulesza RJ, Jr & Berrebi AS (2006). Neurons in the medial nucleus of the trapezoid body and superior paraolivary nucleus of the rat may play a role in sound duration coding. *J Neurophysiol* **95**, 1499–1508.

Kajikawa Y, Saitoh N & Takahashi T (2001). GTP-binding protein bg subunits mediate presynaptic calcium current inhibition by $GABA_B$ receptor. *Proc Natl Acad Sci U S A* **98**, 8054–8058.

Kim JH & von Gersdorff H (2012). Suppression of spikes during posttetanic hyperpolarization in auditory neurons: the role of temperature, I_h currents, and the Na^+-K^+-ATPase pump. *J Neurophysiol* **108**, 1924–1932.

Kimura M, Saitoh N & Takahashi T (2003). Adenosine A1 receptor-mediated presynaptic inhibition at the calyx of Held of immature rats. *J Physiol* **553**, 415–426.

Kirmse K & Kirischuk S (2006). Ambient GABA constrains the strength of GABAergic synapses at Cajal-Retzius cells in the developing visual cortex. *J Neurosci* **26**, 4216–4227.

Koike-Tani M, Kanda T, Saitoh N, Yamashita T & Takahashi T (2008). Involvement of AMPA receptor desensitization in short-term synaptic depression at the calyx of Held in developing rats. *J Physiol* **586**, 2263–2275.

Kombian SB, Zidichouski JA & Pittman QJ (1996). $GABA_B$ receptors presynaptically modulate excitatory synaptic transmission in the rat supraoptic nucleus *in vitro*. *J Neurophysiol* **76**, 1166–1179.

Kontro P & Oja SS (1990). Interactions of taurine with $GABA_B$ binding sites in mouse brain. *Neuropharmacology* **29**, 243–247.

Kopp-Scheinpflug C, Tolnai S, Malmierca MS & Rübsamen R (2008). The medial nucleus of the trapezoid body: comparative physiology. *Neuroscience* **154**, 160–170.

Korogod N, Lou X & Schneggenburger R (2005). Presynaptic Ca^{2+} requirements and developmental regulation of posttetanic potentiation at the calyx of Held. *J Neurosci* **25**, 5127–5137.

Le Feuvre Y, Fricker D & Leresche N (1997). $GABA_A$ receptor-mediated IPSCs in rat thalamic sensory nuclei: patterns of discharge and tonic modulation by GABAB autoreceptors. *J Physiol* **502**, 91–104.

Leão RM & von Gersdorff H (2002). Noradrenaline increases high-frequency firing at the calyx of Held synapse during development by inhibiting glutamate release. *J Neurophysiol* **87**, 2297–2306.

Lee JS, Ho W-K & Lee S-H (2012). Actin-dependent rapid recruitment of reluctant synaptic vesicles into a fast-releasing vesicle pool. *Proc Natl Acad Sci U S A* **109**, E765–774.

Lei S & McBain CJ (2003). $GABA_B$ receptor modulation of excitatory and inhibitory synaptic transmission onto rat CA3 hippocampal interneurons. *J Physiol* **546**, 439–453.

Lerma J, Herranz AS, Herreras O, Abraira V & Martín del Rio R (1986). *In vivo* determination of extracellular concentration of amino acids in the rat hippocampus. A method based on brain dialysis and computerized analysis. *Brain Res* **384**, 145–155.

Lim R, Alvarez FJ & Walmsley B (2000). GABA mediates presynaptic inhibition at glycinergic synapses in a rat auditory brainstem nucleus. *J Physiol* **525**, 447–459.

Lin HH & Dun NJ (1998). Post- and presynaptic $GABA_B$ receptor activation in neonatal rat rostral ventrolateral medulla neurons *in vitro*. *Neuroscience* **86**, 211–220.

Lipstein N, Sakaba T, Cooper BH, Lin K-H, Strenzke N, Ashery U, Rhee J-S, Taschenberger H, Neher E & Brose N (2013). Dynamic control of synaptic vesicle replenishment and short-term plasticity by Ca-calmodulin-Munc13–1 signalling. *Neuron* **79**, 82–96.

Löhrke S, Srinivasan G, Oberhofer M, Doncheva E & Friauf E (2005). Shift from depolarizing to hyperpolarizing glycine action occurs at different perinatal ages in superior olivary complex nuclei. *Eur J Neurosci* **22**, 2708–2722.

Lorteije JAM & Borst JGG (2011). Contribution of the mouse calyx of Held synapse to tone adaptation. *Eur J Neurosci* **33**, 251–258.

Lorteije JAM, Rusu SI, Kushmerick C & Borst JGG (2009). Reliability and precision of the mouse calyx of Held synapse. *J Neurosci* **29**, 13770–13784.

Lu T, Rubio ME & Trussell LO (2008). Glycinergic transmission shaped by the corelease of GABA in a mammalian auditory synapse. *Neuron* **57**, 524–535.

Malitschek B, Rüegg D, Heid J, Kaupmann K, Bittiger H, Fröstl W, Bettler B & Kuhn R (1998). Developmental changes of agonist affinity at $GABA_{BR1}$ receptor variants in rat brain. *Mol Cell Neurosci* **12**, 56–64.

Minelli A, DeBiasi S, Brecha NC, Zuccarello LV & Conti F (1996). GAT-3, a high-affinity GABA plasma membrane transporter, is localized to astrocytic processes, and it is not confined to the vicinity of GABAergic synapses in the cerebral cortex. *J Neurosci* **16**, 6255–6264.

Mizutani H, Hori T & Takahashi T (2006). 5-HT_{1B} receptor-mediated presynaptic inhibition at the calyx of Held of immature rats. *Eur J Neurosci* **24**, 1946–1954.

Moore JK & Moore RY (1987). Glutamic acid decarboxylase-like immunoreactivity in brainstem auditory nuclei of the rat. *J Comp Neurol* **260**, 157–174.

Mukherjee RS, McBride EW, Beinborn M, Dunlap K & Kopin AS (2006). Point mutations in either subunit of the $GABA_B$ receptor confer constitutive activity to the heterodimer. *Mol Pharmacol* **70**, 1406–1413.

Neher E & Sakaba T (2008). Multiple roles of calcium ions in the regulation of neurotransmitter release. *Neuron* **59**, 861–872.

Pírez N & Wachowiak M (2008). *In vivo* modulation of sensory input to the olfactory bulb by tonic and activity-dependent presynaptic inhibition of receptor neurons. *J Neurosci* **28**, 6360–6371.

Portzehl H, Caldwell PC & Rüegg JC (1964). The dependence of contraction and relaxation of muscle fibres from the crab *Maia squinado* on the internal concentration of free calcium ions. *Biochim Biophys Acta* **79**, 581–591.

Renden R, Taschenberger H, Puente N, Rusakov DA, Duvoisin R, Wang L-Y, Lehre KP & von Gersdorff H (2005). Glutamate transporter studies reveal the pruning of metabotropic glutamate receptors and absence of AMPA receptor desensitization at mature calyx of Held synapses. *J Neurosci* **25**, 8482–8497.

Ribak CE, Tong WMY & Brecha NC (1996). GABA plasma membrane transporters, GAT-1 and GAT-3, display different distributions in the rat hippocampus. *J Comp Neurol* **367**, 595–606.

Rodriguez-Contreras A, van Hoeve JS, Habets RLP, Locher H & Borst JGG (2008). Dynamic development of the calyx of Held synapse. *Proc Natl Acad Sci U S A* **105**, 5603–5608.

Roth FC & Draguhn A (2012). GABA metabolism and transport: effects on synaptic efficacy. *Neural Plast* **2012**, 805830.

Sakaba T & Neher E (2003). Direct modulation of synaptic vesicle priming by $GABA_B$ receptor activation at a glutamatergic synapse. *Nature* **424**, 775–778.

Saransaari P & Oja SS (2006). Characteristics of taurine release in slices from adult and developing mouse brain stem. *Amino Acids* **31**, 35–43.

Sätzler K, Söhl LF, Bollmann JH, Borst JGG, Frotscher M, Sakmann B & Lübke JHR (2002). Three-dimensional reconstruction of a calyx of Held and its postsynaptic principal neuron in the medial nucleus of the trapezoid body. *J Neurosci* **22**, 10567–10579.

Schneggenburger R, Meyer AC & Neher E (1999). Released fraction and total size of a pool of immediately available transmitter quanta at a calyx synapse. *Neuron* **23**, 399–409.

Schneggenburger R, Sakaba T & Neher E (2002). Vesicle pools and short-term synaptic depression: lessons from a large synapse. *Trends Neurosci* **25**, 206–212.

Sommer I, Lingenhöhl K & Friauf E (1993). Principal cells of the rat medial nucleus of the trapezoid body: an intracellular *in vivo* study of their physiology and morphology. *Exp Brain Res* **95**, 223–239.

Sonntag M, Englitz B, Kopp-Scheinpflug C & Rübsamen R (2009). Early postnatal development of spontaneous and acoustically evoked discharge activity of principal cells of the medial nucleus of the trapezoid body: an *in vivo* study in mice. *J Neurosci* **29**, 9510–9520.

Sonntag M, Englitz B, Typlt M & Rübsamen R (2011). The calyx of Held develops adult-like dynamics and reliability by hearing onset in the mouse *in vivo*. *J Neurosci* **31**, 6699–6709.

Spirou GA, Brownell WE & Zidanic M (1990). Recordings from cat trapezoid body and HRP labelling of globular bushy cell axons. *J Neurophysiol* **63**, 1169–1190.

Takahashi T, Kajikawa Y & Tsujimoto T (1998). G-protein-coupled modulation of presynaptic calcium currents and transmitter release by a $GABA_B$ receptor. *J Neurosci* **18**, 3138–3146.

Tan ML & Borst JGG (2007). Comparison of responses of neurons in the mouse inferior colliculus to current injections, tones of different durations, and sinusoidal amplitude-modulated tones. *J Neurophysiol* **98**, 454–466.

Taschenberger H, Leão RM, Rowland KC, Spirou GA & von Gersdorff H (2002). Optimizing synaptic architecture and efficiency for high-frequency transmission. *Neuron* **36**, 1127–1143.

Taschenberger H, Scheuss V & Neher E (2005). Release kinetics, quantal parameters and their modulation during short-term depression at a developing synapse in the rat CNS. *J Physiol* **568**, 513–537.

Taschenberger H & von Gersdorff H (2000). Fine-tuning an auditory synapse for speed and fidelity: developmental changes in presynaptic waveform, EPSC kinetics, and synaptic plasticity. *J Neurosci* **20**, 9162–9173.

Tombaugh GC & Somjen GG (1996). Effects of extracellular pH on voltage-gated Na^+, K^+ and Ca^{2+} currents in isolated rat CA1 neurons. *J Physiol* **493**, 719–732.

Tossman U, Jonsson G & Ungerstedt U (1986). Regional distribution and extracellular levels of amino acids in rat central nervous system. *Acta Physiol Scand* **127**, 533–545.

Tritsch NX, Rodríguez-Contreras A, Crins TTH, Wang HC, Borst JGG & Bergles DE (2010). Calcium action potentials in hair cells pattern auditory neuron activity before hearing onset. *Nat Neurosci* **13**, 1050–1052.

Varela JA, Sen K, Gibson J, Fost J, Abbott LF & Nelson SB (1997). A quantitative description of short-term plasticity at excitatory synapses in layer 2/3 of rat primary visual cortex. *J Neurosci* **17**, 7926–7940.

von Gersdorff H & Borst JGG (2002). Short-term plasticity at the calyx of Held. *Nature Rev Neurosci* **3**, 53–64.

Wu L-G, Borst JGG & Sakmann B (1998). R-type Ca^{2+} currents evoke transmitter release at a rat central synapse. *Proc Natl Acad Sci U S A* **95**, 4720–4725.

Wu LG & Borst JGG (1999). The reduced release probability of releasable vesicles during recovery from short-term synaptic depression. *Neuron* **23**, 821–832.

Wu SH & Kelly JB (1991). Physiological properties of neurons in the mouse superior olive: membrane characteristics and postsynaptic responses studied *in vitro*. *J Neurophysiol* **65**, 230–246.

Wu SH & Kelly JB (1995). Inhibition in the superior olivary complex: pharmacological evidence from mouse brain slice. *J Neurophysiol* **73**, 256–269.

Wu Y, Wang H-Y, Lin C-C, Lu H-C, Cheng S-J, Chen C-C, Yang H-W & Min M-Y (2011). $GABA_B$ receptor-mediated tonic inhibition of noradrenergic A7 neurons in the rat. *J Neurophysiol* **105**, 2715–2728.

Yoon K-W & Rothman SM (1991). The modulation of rat hippocampal synaptic conductances by baclofen and γ-aminobutyric acid. *J Physiol (Lond)* **442**, 377–390.

Additional information

Competing interests

None.

Author contributions

T.W., S.I.R., B.H., R.T. and J.G.G.B. designed the experiments. T.W. and B.H. performed *in vivo* experiments, S.I.R. slice experiments; T.W., S.I.R., B.H. and J.G.G.B. analysed the data; T.W., S.I.R. and J.G.G.B. wrote the manuscript. All authors approved the final version.

Funding

This work was supported by an FP6 European Union grant (EUSynapse) and by the Dutch Fund for Economic Structure Reinforcement (FES, 0908 'NeuroBasic PharmaPhenomics project') to J.G.G.B. and a grant from the Grant Agency of the Czech Republic (P303/11/0131) to R.T.

Acknowledgements

We thank C. Donkersloot for help with LabView programming, and Michael Pecka and Eke Bakker for advice on dissolving CGP54626.

Author's present address

S. I. Rusu: University of Amsterdam, Swammerdam Institute for Life Sciences, Center for Neuroscience, Amsterdam, The Netherlands.